

## Interfacial roughness, correlation length, and giant magnetoresistances in NiFeCo/Cu superlattices

Z. T. Diao, K. Meguro, and S. Tsunashima

*Department of Electronics, Nagoya University, Nagoya, 464-01 Japan*

M. Jimbo

*Material Engineering Laboratory, Daido Institute of Technology, Nagoya, 457 Japan*

(Received 12 July 1995; revised manuscript received 10 October 1995)

We have shown by simulating the rocking curve data of x-ray diffraction using diffuse scattering theory that crystalline (111)-oriented NiFeCo/Cu superlattices sputtered on similar NiFeCo buffer layers on glass substrates display substantial correlated interfacial roughness as large as 4–6 Å with moderately large lateral correlation lengths ranging from 180–300 Å. A detailed study of the structures, electronic transport in the field, and magnetization characteristics of the superlattices demonstrated explicitly that under similar conditions of antiferromagnetic coupling giant magnetoresistance increases with increasing interfacial roughness, consistent with the theoretical expectation that giant magnetoresistance is enhanced by the presence of diffuse interface scattering. The experimental results suggest that interfacial roughness chiefly arises from interface disorder at the interfaces.

The subject of giant magnetoresistance has generated a great deal of interest in the correlation between the structure and electronic transport for various superlattice structures since the giant magnetoresistance effect derives from the close proximity of nonmagnetic spacer layers and ferromagnetic layers. Recently, it has been shown that the insertion of ultrathin Co layers into NiFe/Cu superlattices enhances magnetoresistance significantly, which indicates the crucial role of spin-dependent scattering of electrons at the interfaces in determining magnetoresistance.<sup>1</sup> Theoretical results predict a magnetoresistance increasing with diffuse interface scattering.<sup>2</sup> One of the essential ingredients that is concerned with interfaces and can affect the giant magnetoresistance is interfacial roughness. In earlier studies of interfacial roughness, for spin-valve structures that show giant magnetoresistances, no assessment has been made of the correlation between interfacial roughness and the giant magnetoresistance.<sup>3</sup> *A priori*, it is not clear to what extent giant magnetoresistance depends on interfacial roughness. More recently, Fullerton *et al.* has shown that giant magnetoresistance is enhanced by the presence of interfacial roughness in Fe/Cr superlattices.<sup>4</sup> In contrast, other experimental results indicating that giant magnetoresistance decreased with increasing interfacial roughness in the same superlattices have also been reported.<sup>5</sup> These two findings seem to be a matter of controversy. In fact structure and interfacial roughness of superlattices are sensitive to the manufacturing method and other growth parameters including substrate material and/or the presence of initial buffer layers. A further point that may be important is that the interpretation of interfacial roughness and its correlation with magnetoresistance depends on the model one uses. In general interfacial roughness would be a measure of the intricate interaction of x rays with the fluctuations of modulation period<sup>6</sup> and interfacial roughness (e.g., interface disorder<sup>7</sup> and/or composition mixing<sup>8</sup>) existing in those superlattices, not so simple as it was treated in previous work.<sup>4</sup> More detailed examination of experiments is needed. Takanashi *et al.*<sup>5</sup> has given a quantitative description

of interfacial roughness using the modified paracrystalline model. Neglecting the diffuse scattering term and using a small interfacial roughness approximation in this model, however, may invalidate the applicability of this model to the realistically rougher interface structure of a superlattice that shows strong diffuse interface scattering. In this paper, we present for NiFeCo/Cu superlattices a detailed interpretation of small-angle x-ray diffraction and extract interfacial roughness by simulating the rocking curve data using diffuse scattering theory. A further inspection of the complementary magnetic data shows that magnetoresistance increases with increasing interfacial roughness for the superlattices with approximately the same antiferromagnetic coupling.

The specimens used in this experiment were prepared by rf magnetron sputtering with a base pressure of  $<4 \times 10^{-7}$  Torr. The sputtering gas was Ar with a typical value of the partial pressure during deposition of 5 mTorr. The resultant growth rates are 0.74–1.05 and 1.27–1.63 Å/s for magnetic and spacer layer, respectively (see Table I). All of the specimens, with a nominal structure of the form  $[\text{NiFeCo}(15 \text{ \AA})/\text{Cu}(21\text{--}22 \text{ \AA})]_{20}$ , were grown on 50-Å-thick NiFeCo buffer layers on glass substrates at ambient temperature. The (111) orientation of the NiFeCo/Cu superlattices were thoroughly confirmed with the grain sizes of 170–190 Å by high-angle x-ray diffraction, consistent with the results of sectional TEM analysis in our previous work.<sup>9</sup>

Figure 1 shows the magnetoresistance versus field curves measured in the hard in-plane direction of magnetization at room temperature by a four-lead resistivity method for a set of NiFeCo(50 Å)/[NiFeCo(15 Å)/Cu(21–22 Å)]<sub>20</sub> superlattices. The thickness of the spacer layer corresponds to the second antiferromagnetic peak in the spacer-layer dependence of magnetic coupling. One can see that, although the superlattices have nearly the same nominal structure, there is still a scatter in magnetoresistance from specimen to specimen. Note that fluctuations in the sputtering gas pressure and sputtering power during the process of producing the superlattices will result in variations in interfacial roughness. The

TABLE I. Summary of the growth parameters and results of fitting the second-order rocking curves and the magnetic measurements. Interfacial roughness,  $\sigma$ , and lateral correlation length,  $\xi$ , along with the magnetoresistance (MR), are shown for each specimen appearing in Figs. 1 and 3.

Specimens	Dep. rate ( $\text{\AA}/\text{s}$ )		$\sigma$ ( $\text{\AA}$ )	$\xi$ ( $\text{\AA}$ )	MR ratio (%)
	(NiFeCo/Cu)				
A	0.99/1.63		4.24	307	5.7
B	0.74/1.27		5.49	180	8.5
C	1.05/1.34		5.57	221	9.4
D	0.96/1.58		5.64	240	11.6

changes in magnetoresistance can be tentatively correlated to the interfacial roughness being examined below.

In Fig. 2(a) typical small-angle  $(\theta, 2\theta)$  curves of x-ray diffraction taken in the specular geometry and with the specimen rotated  $0.2^\circ$  off specular [offset  $(\theta, 2\theta)$  curve] are plotted for the specimen with a smaller magnetoresistance [Fig. 1(a)]. In Fig. 2(b) a similar set of curves is plotted for the specimen with a larger magnetoresistance [Fig. 1(c)]. For the data sets taken in the specular geometry, each of them exhibits distinguishable superlattice Bragg peaks up to the second order and many small, clean-cut finite-size peaks between the two Bragg peaks arising from the interference of x-ray reflections from superlattice surface and film-substrate surface. It seems that for the specimen that has a larger magnetoresistance the intensity is reduced for the first peak but not for the second peak. None of our small-angle diffraction data indicates a clear trend of the suppression of the intensity or the broadening of the Bragg peaks as the interface imperfection increases, as was reported by Fullerton *et al.*<sup>4</sup> Both of the offset  $(\theta, 2\theta)$  curves in the figure show that the diffuse intensity has the same  $S_z$  dependence as the specular intensity, but grows with increasing order relative to the specular intensity. This peaking of the diffuse intensity in  $S_z$  at the Bragg condition implies that the vertically correlated roughness is present to be a dominant one in these superlattices

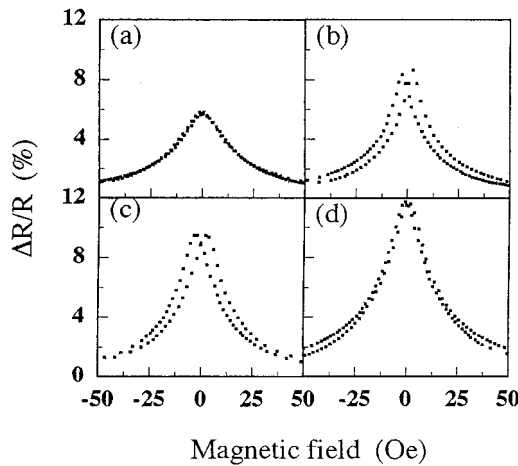


FIG. 1. Resistance vs in-plane field measured in the hard direction of in-plane magnetization at 295 K for a set of specimens (a)–(d) with a nominal structure of the form NiFeCo(50  $\text{\AA}$ )/[NiFeCo(15  $\text{\AA}$ )/Cu(21–22  $\text{\AA}$ )]<sub>20</sub>. The interface imperfections can be responsible for the scatter in their values.

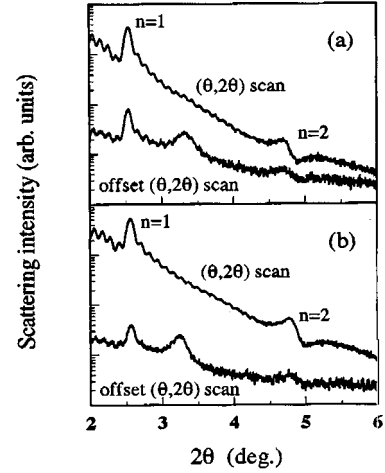


FIG. 2. Diffracted intensity (a) and (b) for two geometries; normal and offset- $(\theta, 2\theta)$  scans with a  $0.2^\circ$  offset angle for the specimens shown in Figs. 1(a) and 1(c).

because for a perfect vertical correlation of roughness all the diffuse intensity is confined to the  $S_x, S_y$  plane at the Bragg condition  $S_z = 2\pi n/d$ . The main peak located between the first and second Bragg peaks reflects a strong diffuse scattering of x rays from buffer layer in the superlattice. The explanation of the exact nature of this interface imperfection needs some model fits to the data. Generally, the scattering of x rays from a rough surface/interface can be split into specular reflection and diffuse scattering terms and described as self-affine over finite length scales calculated in the first Born approximation.

In the case of superlattices, interfacial roughness can be characterized as either being correlated between layers or being random. The degree of interfacial roughness correlation for the former depends on its lateral length scale, with the correlation becoming random at short scale. Indirect evidence that large-scale substrate roughness can be propagated through these superlattice structures has been also obtained from the results of high-resolution TEM analysis in our previous work.<sup>9</sup> The amount of roughness at the various interfaces is reflected by the total diffusely scattered intensity while the degree of correlation present is determined by its distribution in reciprocal space. An estimate of the lateral length scale of the vertically correlated roughness can be obtained from rocking curves. For a single rough surface, the scattered intensity per unit area can be written as<sup>10</sup>

$$I(S) = I_0 \exp(-S_z^2 \sigma^2) / S_z^2 \int \int dX dY \exp[S_z^2 C(X, Y)] \times \exp[-i(S_x X + S_y Y)], \quad (1)$$

where  $I_0$  is the intensity per unit area of the incident beam,  $X, Y$  the components of the lateral separation of two points on the surface, and  $\sigma$  the rms roughness. Assuming that for two points on a surface separated by some small distance  $R = (X^2 + Y^2)^{1/2}$ , the correlation function

$$C(X, Y) = \langle z(r)z(r-R) \rangle = \sigma^2 \exp[-(R/\xi)^{2h}] \quad (2)$$

is obtained, in which  $z(r)$  is the vertical displacement of the surface from its average height at the site defined by the lateral coordinate  $r$ ,  $\xi$  is the lateral correlation length, and  $h$

is related to the fractal dimension and equal to  $1/2$ . Inserting this correlation function into the scattered intensity formula gives

$$I(S_x, S_z) = 2\pi I_0 \exp(-S_z^2 \sigma^2) / S_z^2 \left[ 2\pi \delta(S_x) + \sum_{m=1}^{\infty} \frac{2\xi(S_z^2 \sigma^2)^m}{m(m!)} \frac{1}{(1 + S_x^2 \xi^2 / m^2)} \right], \quad (3)$$

where this integration is realized experimentally by detecting the scattered x rays with a sufficiently long slit. The intensity is separated into two terms, a  $\delta$  function and a diffuse term. The diffuse intensity due to scattering off the disorder has a shape that depends on the scatter-scatter correlation in the direction measured. The extension of this result to the case of superlattices, in which vertical correlated roughness at interfaces prevails, is straightforward if the average layer spacing does not change throughout the thickness of the superlattices.<sup>11</sup> The modified result, therefore, is simply a product of the intensity scattered by a single rough surface and the reflectivity of the perfect stack.

In the rocking curve geometry with a Cu  $K\alpha$  wavelength of  $1.54 \text{ \AA}$ ,  $2\theta$  is held fixed and  $\omega$  is varied, where  $2\theta$  is the angle between the source and detector and  $\omega$  is the angle between source and specimen. Through the use of a narrow entrance slit to the detector, the diffraction measurement profiles an angular distribution of the x rays in a cut perpendicular to the surface normal, a sharp central spike above a slowly varying diffuse background. This instrument-limited spike is representative of true specular reflection of the x rays from the superlattice. All of the rocking curve data were multiplied by  $\sin \omega / \sin \theta$  to correct the asymmetry effect resulting from the change in the volume of the specimen being probed. The essential procedure used to fit the rocking curve follows what was done by Savage *et al.*<sup>11</sup> The theoretical profile is obtained by multiplying Eq. (3) with an envelope function that corrects for two geometrical factors then convoluted with a function representing the instrumental broadening. The first geometrical factor arises from the change in beam attenuation with  $\omega$  that arises because of the change in the path length the x rays travel and the second from attenuation of the measured intensity at the extremes of the rocking curve due to the effect of the cut through reciprocal space a rocking curve makes. Experimentally the instrumental broadening was determined only as a form of its upper limit from the first-order rocking curve by subtracting the diffuse background. Convoluting this function with the theoretical profile results in the sum of an instrument-limited central spike and a diffuse component that is relatively unchanged.

We deal with the second-order rocking curve to extract interfacial roughness and lateral correlation length because the diffuse component becomes relatively stronger with increasing order and the result obtained from fitting the higher orders represents more of an average interfacial roughness in the bulk of the superlattices instead of interface and/or surface roughness near the outer surface of the specimen. The second-order rocking curve data and corresponding fits for these specimens with a nominal structure of the form  $\text{Ni-FeCo} (50 \text{ \AA}) / [\text{NiFeCo}(15 \text{ \AA}) / \text{Cu}(21\text{--}22 \text{ \AA})]_{20}$  are plotted in Fig. 3. The results of rocking-curve fitting for all specimens are summarized in Table I. It is shown that all these speci-

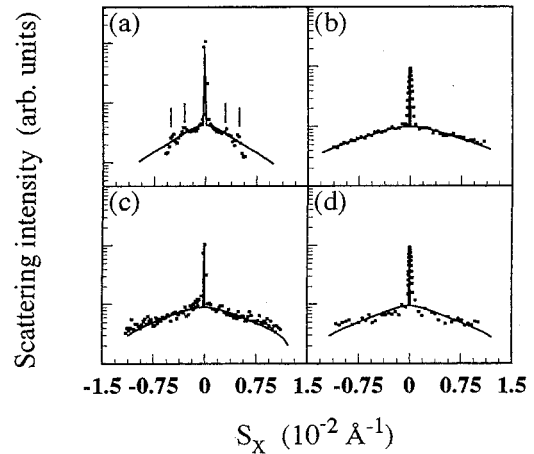


FIG. 3. Second-order rocking curves (dotted lines) obtained from the specimens (a)–(d) shown in Fig. 1 and calculated fits (solid lines) using  $h=1/2$  and the parameters of interfacial roughness and lateral correlation length shown in Table I. Also shown in (a) are the rocking-curve satellites due to the double diffraction.

mens have relatively large correlated interfacial roughness  $\sim 4\text{--}6 \text{ \AA}$ , implying the possibility that substrate roughness is replicated by the deposited overlayers. It suggests that substrate affects the nucleation of initial layer (buffer layer) and the change occurring in initial layer is in turn replicated during the rest of growth. The lateral correlation length of the propagated roughness is estimated to be  $\sim 180\text{--}300 \text{ \AA}$  for these superlattices. It is clear that for a small value of  $\xi$  the diffuse intensity is spread into a large angle, thus reducing its contribution near the specular direction. If the lateral correlation lengths are much smaller than the wavelength of the scattered wave, they will not contribute to the diffused reflectivity. With its moderately large lateral correlation length correlated roughness is hence expected to play an important role in determining electronic transport properties such as the magnetoresistance in these superlattices which is largely determined by the spin-dependent specular- and diffuse-scattering behavior of electrons at interfaces. For the rocking curve shown in Fig. 3(a), we observed extra peaks (or valleys) with twofold symmetry about the central peak. The presence of these satellites can be understood in terms of double diffraction. Because the scattered intensity due to both the singly scattered second-order and the doubly scattered first-order beams leave the specimen at the same angle, the interference of these two beams gives the extra feature at this diffraction condition.

Shown in Fig. 4 are the in-plane magnetization curves measured in the hard direction of magnetization for the specimens appeared in Figs. 1 and 3. They show the characteristic shearing and low remanent moment arising from the antiferromagnetic coupling amongst magnetic layers. The rougher specimen has a decreasing remanent moment due to a stronger antiferromagnetic coupling increasing the magnetoresistance. Moreover, there is a trace that the saturation moment increases somewhat with interfacial roughness from specimen to specimen with a small amount two orders of magnitude smaller than the saturation moment itself. The question is whether it implies that interdiffusion at the interfaces is weaker for the rougher specimens with a larger magnetoresistance than the “smoother” one. Note that interdiffusion at interfaces in NiFe/Cu/NiFe spin valve structures

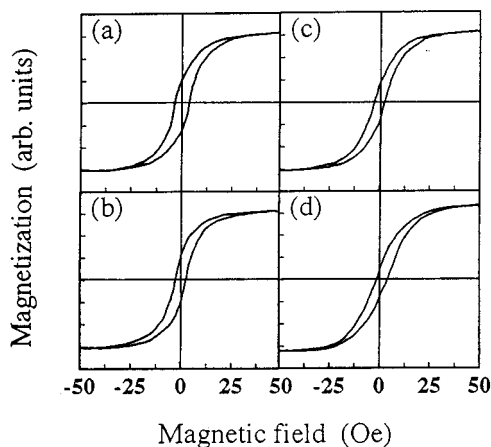


FIG. 4. Magnetization curves measured at 295 K in the hard in-plane direction for the specimens (a)–(d) shown in Fig. 1.

has been found to create a thin paramagnetic interfacial region at interface that reduces the saturation moment and alters electronic transport.<sup>12</sup> Similar performances of the magnetically inactive region at interfaces originating from interdiffusion have been observed in <sup>59</sup>Co nuclear magnetic resonance (NMR) spin-echo studies of Co/Cu superlattices where the compositional mixing at interfaces plays a role to decrease the saturation moment and magnetoresistance in those superlattices.<sup>13</sup> At the present stage, although the details of interdiffusion at interfaces and exactly to what extent it has evolved remain unclear for our superlattices, the compositional mixing of Cu and Ni atoms through interdiffusion, if occurred, is most likely to progress first at interfaces and their alloying then reduces the saturation moment of the superlattices following the formation of thin paramagnetic interfacial region.<sup>14,15</sup> In addition, interdiffusions amongst the atoms of other constituents involved, of course, are still possible and expected to lead to similar results. Values of the saturation moment for the superlattices and NiFeCo alloy film ( $4\pi Ms \sim 1.17 \times 10^4$  Gs) can provide an approximate measure of interdiffusion at interfaces. Suppose that interdiffusive mixing regions at interfaces are magnetically inactive; approximately, we estimated in our superlattices the interdiffusive region not to be more than 2–3 atomic monolayers in width. The result is in quantitative agreement with the greatness of interfacial roughness determined by the x-ray diffraction mentioned above, while for rougher specimens we also see a suppression of the development of the interdiffusive

region which, for instance, amounts to only one monolayer thick for the roughest specimen. It is hence evident that the reason that caused the saturation moment to increase in rougher specimens can be accounted for by the reduction in thickness of magnetically inactive interdiffusive region at interfaces. Also one of the other possible sources for this could be an increment of local magnetic moments on magnetic and/or nonmagnetic atoms due to significant modification in electronic and magnetic structures near interfaces as the degree of interfacial disorder is enhanced.<sup>16</sup>

Of topographical interface disorder and interdiffusion we may ask which we have dealt with so far dominates interfacial roughness. In case interfacial roughness be attributed to interdiffusion at interfaces, there should be consequently an increase in thickness of the interdiffusive region then a decrease in the saturation moment of the superlattices with increasing interfacial roughness. However, the expectation is contrary to the experiments that the saturation moment increases even a little when interfacial roughness increases. We take it to indicate that topographical interface disorder duplicated from buffer layer and/or substrate, but not interdiffusion at interfaces, should be predominantly responsible for interfacial roughness than its correlation with magnetoresistance in question. A further comparison of the data of structure and magnetoresistance in Table I displays that for the specimens with approximately the same antiferromagnetic coupling giant magnetoresistance insists on getting larger with increasing interfacial roughness. This agrees qualitatively with the theoretical results that the spin-dependent random potential at interface<sup>16–18</sup> or spin-dependent diffuse interface scattering<sup>2</sup> enhances the magnetoresistance.

In summary we have shown that highly oriented (111) NiFeCo/Cu superlattices sputtered on NiFeCo buffer layers on glass substrates display substantial correlated interfacial roughness as large as 4–6 Å with moderately large lateral correlation length scale  $\xi$  ranging from 180 to 300 Å. The result that correlated roughness remains almost constant throughout the film thickness suggests that these superlattices are neither smoothing nor roughening appreciably over the lateral length of correlated roughness. Interfacial roughness chiefly arises from topographical interface disorder at interfaces. The giant magnetoresistance for nearly the same magnetic coupling increases as interfacial roughness increases.

We would like to thank Y. Kamada and M. Doi for their help during the x-ray-diffraction characterization. S. J. Diao was helpful in computation for part of this work.

<sup>1</sup>S. S. Parkin, *Appl. Phys. Lett.* **61**, 1358 (1992).

<sup>2</sup>R. E. Camley and J. Barnas, *Phys. Rev. Lett.* **63**, 664 (1989).

<sup>3</sup>T. C. Huang *et al.*, *Appl. Phys. Lett.* **60**, 1573 (1989).

<sup>4</sup>E. E. Fullerton *et al.*, *Phys. Rev. Lett.* **68**, 859 (1992).

<sup>5</sup>K. Takanashi *et al.*, *J. Phys. Soc. Jpn.* **61**, 1169 (1992).

<sup>6</sup>Y. Fujii *et al.*, *J. Phys. Soc. Jpn.* **55**, 251 (1986).

<sup>7</sup>J. P. Locquet *et al.*, *Phys. Rev. B* **39**, 13 338 (1989).

<sup>8</sup>F. J. Lamelas *et al.*, *Phys. Rev. B* **43**, 12 296 (1990).

<sup>9</sup>S. Tsunashima *et al.*, in *Magnetic Ultrathin Films—Multilayers and Surfaces, Interfaces and Characterization*, edited by B. T. Jonker *et al.*, MRS Symposia Proceedings No. 313 (Materials

Research Society, Pittsburgh, 1993), p. 271.

<sup>10</sup>S. K. Sinha *et al.*, *Phys. Rev. B* **38**, 2297 (1988).

<sup>11</sup>D. E. Savage *et al.*, *J. Appl. Phys.* **69**, 1411 (1991).

<sup>12</sup>J. P. Nozieres *et al.*, *J. Magn. Magn. Mater.* **121**, 386 (1993).

<sup>13</sup>Y. Saito *et al.*, *J. Phys. Soc. Jpn.* **62**, 1450 (1993).

<sup>14</sup>R. M. Bozorth, *Ferromagnetism* (Van Nostrand, New York, 1951), p. 441.

<sup>15</sup>S. A. Ahern *et al.*, *Proc. R. Soc. London* **248**, 145 (1958).

<sup>16</sup>H. Hasegawa, *J. Phys. Condens. Matter* **4**, 169 (1992).

<sup>17</sup>P. M. Levy *et al.*, *Phys. Rev. Lett.* **65**, 1643 (1990).

<sup>18</sup>J. Inoue *et al.*, *J. Phys. Soc. Jpn.* **60**, 376 (1991).